

# Shamap: Shape-based Manifold Learning

Fenglei Fan, *Student Member, IEEE*, Hongming Shan,  
Ge Wang, *Fellow, IEEE*  
Biomedical Imaging Center, CBIS/BME/SoE  
Rensselaer Polytechnic Institute, Troy, New York, USA

**Abstract**— For manifold learning, it is assumed that high-dimensional sample/data points are on an embedded low-dimensional manifold. Usually, distances among samples are computed to represent the underlying data structure, for a specified distance measure such as the Euclidean distance or geodesic distance. For manifold learning, here we propose a metric according to the angular change along a geodesic line, thereby reflecting the underlying shape-oriented information or the similarity between high- and low-dimensional representations of a data cloud. Our numerical results are described to demonstrate the feasibility and merits of the proposed dimensionality reduction scheme.

**Index Terms** —Manifold learning, dimensionality reduction, similarity measure, feature representation.

## I. INTRODUCTION

HIGH dimensional big data become increasingly important but they are usually difficult to be directly utilized. Fortunately, in many cases such data are essentially low dimensional; i.e., they stay on a low-dimensional manifold embedded in the high dimensional space [1]. This key observation suggests the possibility of dimensionality reduction to facilitate visualization and analysis of the data.

Manifold learning is one of the mainstream nonlinear dimensionality reduction techniques [2]. Driven by major academic and practical motives, many algorithms [3-9] were developed to flatten an embedded manifold and reveal an intrinsic structure. One of the representative methods, Isomap combines the Floyd-Warshall algorithm with multidimensional scaling (MDS [10]) to compress high-dimensional data. The idea behind MDS is to form a configuration of points in a low-dimensional space such that the distances among the points in a high-dimensional space are well preserved. In the framework of Isomap, the geodesic distances, instead of Euclidean distances, are fed into MDS for eigen decomposition.

In MDS, given all the distances between samples, the structure of the dataset can be well characterized. It is not surprising from the perspective of congruent triangle: first, we can randomly select three points from a dataset of interest. By the correspondence between congruent triangles, we can uniquely determine these points if we know mutual distances among three non-collinear points. Next, we can add one additional neighboring point not collinear with two of the selected points, and the new point can be uniquely localized according to its distances to the non-collinear points. So on and so forth, all the

points in the dataset can be uniquely positioned in the high-dimensional space up to a rigid transformation.

Inspired by the Isomap, we are more interested in shape-based manifold learning; i.e., our goal is to map a high-dimensional data cloud to a low-dimensional version so that the shapes in the two presentations are similar. In contrast to the Isomap that is appreciated from the perspective of congruent triangle, what we propose here is called the Shamap under the perspective of similar triangle. In other words, while the Isomap is distance-wise specific, the Shamap is angularly sensitive. Indeed, angular relations are a significant aspect of data structures. For example, a polar coordinate system is often more meaningful and convenient in representing many important curves than a Cartesian coordinate system. Moreover, since the angular increment is perpendicular to the tangential direction of a trajectory, the angular representation is most suitable to capture the shape of the trajectory.

Specifically, we propose to replace the geodesic distance with the accumulated angular changes along a geodesic line in the framework of Isomap to form our proposed algorithm Shamap. We compute the angle between two neighboring vectors by

$$\cos(\theta_{ij}) = (\vec{x}_i - \vec{c}) \cdot (\vec{x}_j - \vec{c}) / (\|\vec{x}_i - \vec{c}\| \cdot \|\vec{x}_j - \vec{c}\|), \quad (1)$$

where  $\vec{c}$  is the global reference for all the points, and the norms of data vectors are used for normalization.

There are multiple methods that reduce the dimensionality of a data cloud while keeping a global structure by posing local restriction, such as Locally Linear Embedding (LLE) and Hessian LLE. Different from them, both Isomap and Shamap compute global structures directly in terms of geodesic distance and geodesic tangential respectively. At the same time, iterative optimization is not needed in Isomap and Shamap compared to those local methods so that the computational cost is reduced. Due to the shape preserving property of Shamap, it is potentially more advantageous in unraveling convoluted structures than Isomap.

In the next section, we describe the Shamap algorithm and compare it with Isomap. In the third section, we evaluate Shamap with numerical examples, including in-house examples and common benchmarks. In the last section, we discuss related issue and conclude the paper.

## II. SHAMAP METHOD

Given a dataset  $\vec{x}_1, \vec{x}_2, \vec{x}_3, \dots, \vec{x}_K$ , the tangential angles at those points are calculated by Eq. (1). The proposed Shamap algorithm consists of the following three steps:

**#1 Find K-nearest neighbors:** Determine whether a pair of points  $i$  and  $j$  are connected or not according to the K-nearest neighbor criterion, or if they are within a fixed distance  $\varepsilon$ .

**#2 Compute the total angular change:** To compute the total angular change  $\theta_{mn}$  between two points  $m$  and  $n$ , first determine the shortest path connecting  $m$  and  $n$ , such as  $(m, k_1, k_2, \dots, k_W, n)$  then  $\theta_{mn}$  is derived by accumulating incremental angular changes along the geodesic line:

$$\theta_{mn} = \theta_{mk_1} + \theta_{k_1k_2} + \dots + \theta_{k_Wn}, \quad (2)$$

where subscripts pairs  $(m, k_1), (k_1, k_2), \dots, (k_W, n)$  denote pairs of neighboring points.

**#3 Construct a  $d$ -dimensional embedding:** Compute *cosine values* of local angular changes to form a matrix  $C$ . Let  $\lambda_p$  be the  $p$ -th eigenvalue of the matrix  $C$  and  $\vec{u}_p$  be the  $i$ -th component of the  $p$ -th eigenvector. Then, the  $p$ -th component of the  $d$ -dimensional coordinate vector  $\vec{y}_i$  is computed as  $\vec{y}_i^p = \sqrt{\lambda_p} \vec{u}_p^i \|\vec{x}_i - \vec{c}\|$ . The scaling factor  $\|\vec{x}_i - \vec{c}\|$  is needed to reasonably distribute the high-dimensional points projected onto the low-dimensional manifold according to the vector norm relative to the reference point  $\vec{c}$ .

## III. NUMERICAL SIMULATIONS

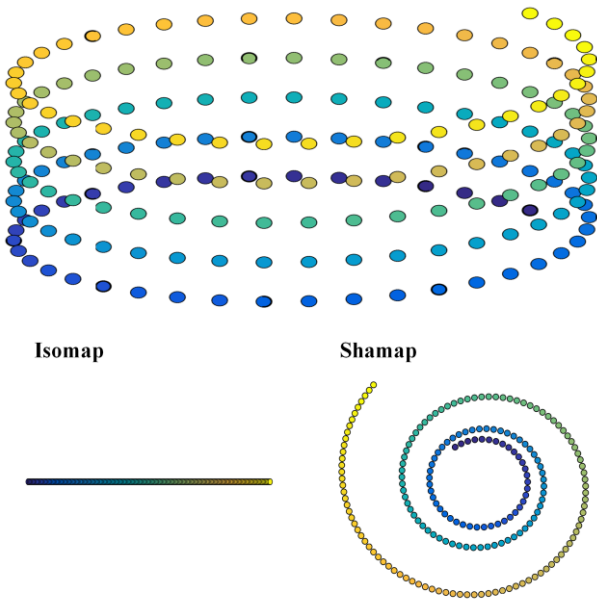


Fig. 1. More shape information is revealed of a helix using Shamap than Isomap. Given the difference in the metric between Isomap and Shamap,

our insight is that Shamap is more shape-friendly. For example, a helix was generated according to the parametric equation:  $x = \cos(t); y = \sin(t); z = 0$ , where  $t$  was varied from 0 to  $10\pi$  with a step size  $0.05\pi$ . That is, we obtained a dataset with 201 samples. Then, we employed Isomap and Shamap respectively to unfold this 3D data cloud onto a 2D manifold with  $\vec{c} = 0$  and  $K = 2$  (Note that all points, except for the starting and end points, have two neighbors), as shown in Figure 1. Visually, Shamap yielded much more relevant structural information than Isomap. For example, the 3D spiral rotation was well sensed in the low-dimensional space, while Isomap degraded the helix into a straight line. Actually, we can roughly estimate the number of helix turns based on the mapped curve.

Based on our above observation, an important application of Shamap would be for high-dimensional visualization. Then, we applied Shamap in visualizing two toy examples and two benchmark datasets.

### A. Protein Unfolding

With advanced Cryo-EM [11], structural biology has made a huge progress over recent years. Determining the structure of a key protein is of great significance for understanding its functions. In the experiments, it is relatively easy to figure out the configurative amino acid sequence but difficult to estimate the high order structural features [12]. Also, protein unfolding is another challenge. Thus, it is meaningful to describe a protein folding configuration in a low-dimensional space [13].

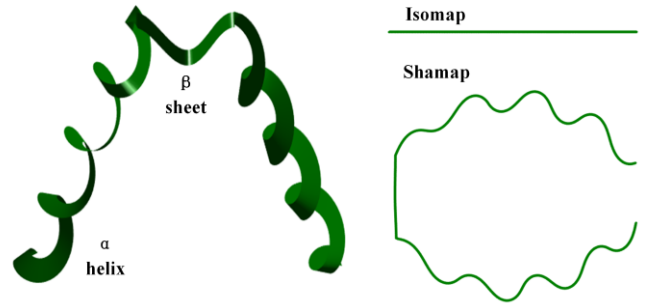


Fig. 2. Protein unfolding using Isomap and Shamap respectively.

Here we look at the protein unfolding problem to show the utility of Shamap. The  $\alpha$  helices and  $\beta$  sheet are very common second order structures of proteins [14]. Without loss of generality, we made a toy protein model consisting of two  $\alpha$  helices joint by a  $\beta$  sheet, where  $\alpha$  helices and  $\beta$  sheet are respectively expressed by the aforementioned equation and a cosine function. Then, we unfolded the protein model with Isomap and Shamap respectively, as shown in Figure 2. It is seen that while Isomap mapped the protein into a straight line as expected, Shamap turned the 3D  $\alpha$  helices into 2D spirals with the  $\beta$  sheet into a straight line in a proper location.

### B. Double Helix Separation

We further evaluated the unique capability of Shamap with a 3D double helix model. The 3D model consists of a pair of parallel helices around a common principle axis. First, we

generated double helix data according to the following equations:

$$\begin{aligned} x_1 &= \cos(t), x_2 = \cos(t + \pi) \\ y_1 &= \sin(t), y_2 = \sin(t + \pi) \\ z_1 &= 0.1t, z_2 = 0.1t \end{aligned}$$

We let  $t$  change from 0 to  $10\pi$  at a step size  $0.05\pi$  as before. We prepared their low dimensional visualizations according to the starting point in the high dimensional space. The final results are in Figure 3. Two helices are respectively denoted in red cross and blue circle. While the helices were superimposed together in the Isomap presentation, the Shamap representation separated them well.

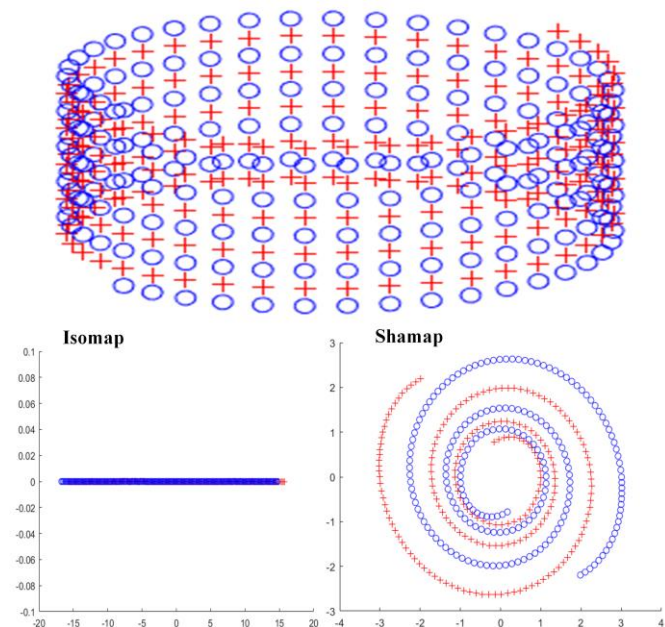


Fig. 3. Dimensionality reduction for 3D helices using Isomap and Shamap respectively.

### C. MNIST

In addition to the above toy examples, we also tested the utility of Shamap with public benchmarks. Shamap was used to process 250 “0” (blue circle) and 250 “1” images (red cross). The parameters were  $\vec{c}=0, K=20$ . As shown in Figure 5, Shamap not only separated the two digits well but also differentiated shape variations of the “0” and “1” images very reasonably. For example, zeros were mapped into a “ball” and ones were scattered in a “fan”. Moreover, a detailed inspection reveals that Shamap sorted images orientation-wise: the orientation of “1” changed gradually along the shape of the fan, with the light and high contrast digits inside and outside respectively, as shown in Fig. 5. In contrast, the Isomap transform produced the map where the thickness of “1”s became gradually less from the left to right but “different orientations of these “1”s were still mixed together. In Figure 6, 1,000 “1” images were processed to highlight this trend, with the parameters  $\vec{c}=0, K=5$ .

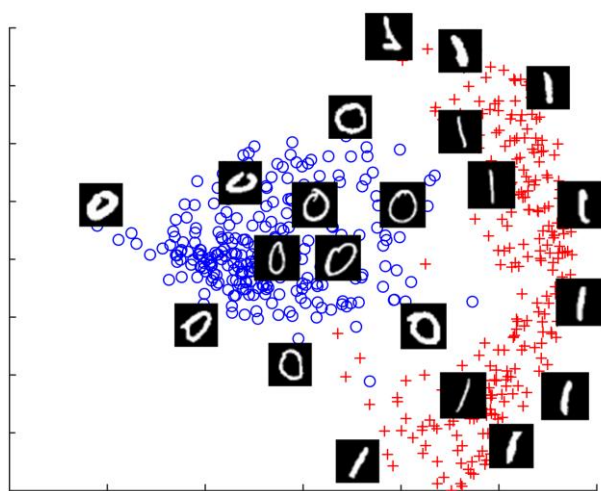


Fig. 4. 250 “0” (blue circle) and “1” (red cross) images were analyzed using Shamap.

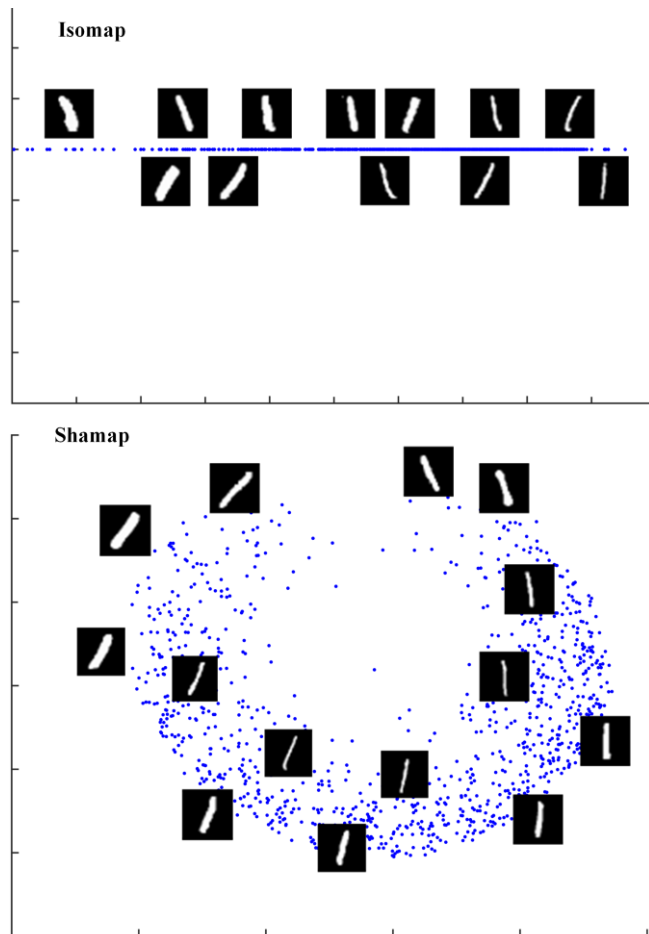


Fig. 5. 1,000 “1” images were analyzed using Shamap.

### D. COIL-20

The Sammon mapping is a most popular nonlinear dimension reduction method. Figure 7 shows the results of applying Shamap and Sammon mapping to the COIL-20 [15] dataset.  $K$  was set to 12. For some of the 20 objects, Shamap separated them apart, which means that the intrinsic representation of those points is essentially one-dimensional. For more complex objects, the extent of aliasing with Shamap is less severe than

that with the Sammon mapping; such as the patterns denoted as black triangle and green circle.

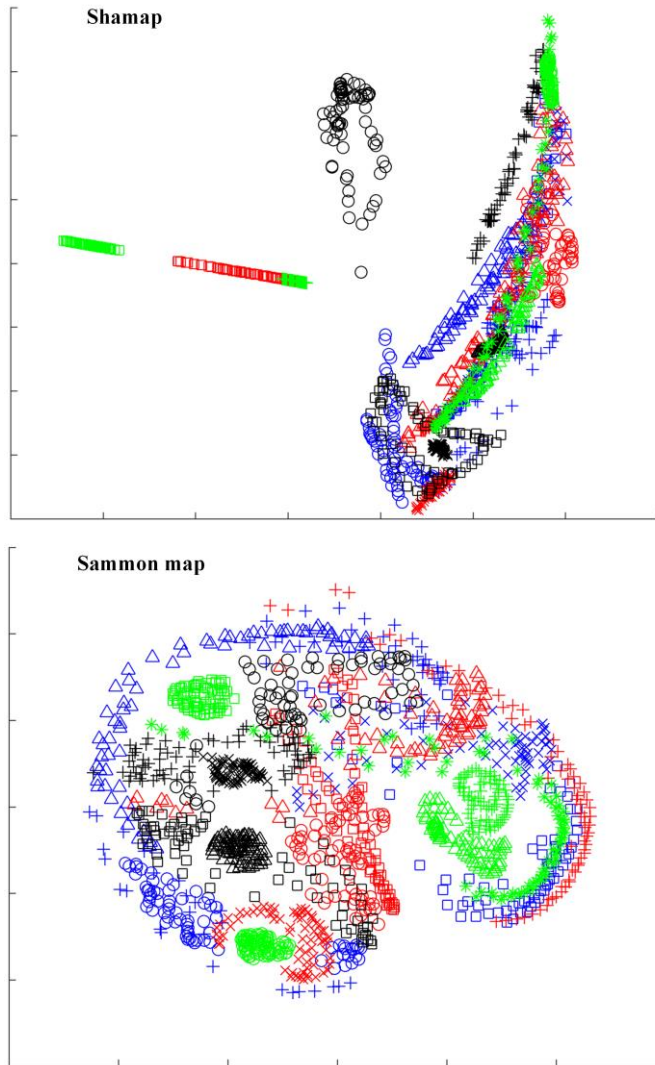


Fig. 6. Dimension deduction for COIL-20 using Shamap and Sammon mapping.

#### IV. DISCUSSIONS AND CONCLUSION

In a neighborhood relation of each point, Isomap computes the geodesic distance between the points on the manifold. In contrast, Shamap measures the accumulated angular change along the geodesic line with respect to a reference point; i.e., angles on the surface of the manifold are calculated. Therefore, Shamap is good at keeping shape information. As illustrated in Figure 2, while Isomap tends to unfold proteins into a straight line, Shamap carries shape differences from the high- to low-dimensional space. An interesting topic is to perform a topology-preserving dimensionality reduction transform. We believe that Shamap is better than Isomap towards this goal.

The manifold sculpting method iteratively finds an embedding by sensing the surface tension of local regions [7]. Manifold sculpting records local angular information in an original high-dimensional space and uses it as one of the constraints to construct a weighted error functional. The philosophy behind this method is that local properties help interpret the global

structure. In our proposed Shamap, the angular information is computed along the geodesic line, giving the global knowledge directly for dimension reduction.

Compared with Isomap, Shamap has the adjustable parameter  $\bar{c}$ , which gives the freedom to enhance the outcome. Although in our studies, we only use  $\bar{c}=0$ , this parameter can be optimized according to some criterion in a task-specific fashion. It is possible to use the machine learning techniques [16] for an optimal  $\bar{c}$ .

Both Isomap and Shamap involve the eigen decomposition in the final step. It is noted that eigen decomposition is sensitive to noise [17-18]. However, the error due to noise could be lower for Shamap than that for Isomap in the cases where the angular change over a long range is more reliable than the distance measure of the geodesic line due to random fluctuations along the geodesic line (see the coastline paradox: [https://en.wikipedia.org/wiki/Coastline\\_paradox](https://en.wikipedia.org/wiki/Coastline_paradox)).

In conclusion, we have proposed a new nonlinear algorithm, Shamap, for dimensionality reduction. The key merit of Shamap is its shape preserving property. Our pilot studies show shape-information-rich results after dimensionality reduction using Shamap, favorably compared with the counterparts obtained using Isomap. Further efforts are in progress to apply Shamap in real-world applications and improve it for topological invariability.

#### REFERENCES

- [1] J. B. Tenenbaum, De V. Silva, J. C. Langford, "A global geometric framework for nonlinear dimensionality reduction," *Science*, vol. 290, no. 5500, pp. 2319-2323, 2000.
- [2] Y. Bengio, A. Courville, P. Vincent, "Representation learning: A review and new perspectives," *IEEE transactions on pattern analysis and machine intelligence*, vol. 35, no. 8, pp. 1798-1828, 2013.
- [3] J. W. Sammon, "A nonlinear mapping for data structure analysis," *IEEE Transactions on computers*, vol. 100, np. 5, pp. 401-409, 1969.
- [4] S. T. Roweis, L. K. Saul, "Nonlinear dimensionality reduction by locally linear embedding," *Science*, vol. 290, no. 5500, pp. 2323-2326, 2000.
- [5] D. L. Donoho, C. Grimes, "Hessian eigenmaps: Locally linear embedding techniques for high-dimensional data," *Proceedings of the National Academy of Sciences*, vol. 100, no. 10, pp. 5591-5596, 2003.
- [6] M. Belkin, P. Niyogi, "Laplacian eigenmaps for dimensionality reduction and data representation," *Neural computation*, vol. 15, no. 6, pp. 1373-1396, 2003.
- [7] M. Gashler, D. Ventura, T. Martinez, "Iterative non-linear dimensionality reduction with manifold sculpting," *Advances in Neural Information Processing Systems*, pp. 513-520, 2008.
- [8] L. Maaten, G. Hinton, "Visualizing data using t-SNE," *Journal of machine learning research*, vol. 9, pp. 2579-2605, 2008.
- [9] Z. Zhang, H. Zha, "Principal manifolds and nonlinear dimensionality reduction via tangent space alignment," *SIAM journal on scientific computing*, vol. 26, no.1, pp. 313-338, 2004.
- [10] J. B. Kruskal, "Multidimensional scaling by optimizing goodness of fit to a nonmetric hypothesis," *Psychometrika*, vol. 29, no. 1, pp. 1-27, 1964.
- [11] M. Liao, E. Cao, D. Julius, et al. "Structure of the TRPV1 ion channel determined by electron cryo-microscopy," *Nature*, vol. 504, no. 7478, pp. 107, 2013.
- [12] M. J. Wood, J. D. Hirst, "Protein secondary structure prediction with dihedral angles," *PROTEINS: Structure, Function, and Bioinformatics*, vol. 59, no. 3, pp. 476-481, 2005.

- [13] P. Das, M. Moll, H. Stamati, et al. "Low-dimensional, free-energy landscapes of protein-folding reactions by nonlinear dimensionality reduction," *Proceedings of the National Academy of Sciences*, vol. 103, no. 26, pp. 9885-9890, 2006.
- [14] D. T. Jones, "Protein secondary structure prediction based on position-specific scoring matrices1," *Journal of molecular biology*, vol. 292, no.2, pp. 195-202, 1999.
- [15] S. A. Nene, S. K. Nayar, H. Murase, "Columbia object image library (coil-20)," 1996.
- [16] Y. LeCun, Y. Bengio, G. Hinton, "Deep learning," *Nature*, vol. 521, no. 7553, pp. 436, 2015.
- [17] Y. Aflalo, R. Kimmel, "Spectral multidimensional scaling," *Proceedings of the National Academy of Sciences*, vol. 110, no. 45, pp. 18052-18057, 2013.
- [18] A. Maćkiewicz, W. Ratajczak, "Principal components analysis (PCA)," *Computers & Geosciences*, vol. 19, no. 3, pp. 303-342, 1993.